Solar Extreme Ultraviolet Heating and Dynamical Processes in the Mid-Latitude Thermosphere

P. AMAYENC

CNET/RSR, Issy-les-Moulineaux, France

D. ALCAYDE

CESR, Toulouse, France

G. KOCKARTS

Institut d'Aéronomie Spatiale, Brussels, Belgium

By using a global pressure gradient model deduced from satellite drag data the momentum and the mass conservation equations are solved to obtain the neutral wind vector at mid-latitude. In this computation the ion drag term is calculated from incoherent scatter measurements at Saint-Santin (France). Then the most important terms of the energy conservation equation are calculated, and the relative importance of dynamical heating processes is deduced and compared with direct EUV heat input. The model used in the computation is roughly consistent with solar EUV heating if vertical and horizontal transport effects are included in the energy balance equation.

INTRODUCTION

A complete description of the terrestrial upper atmosphere requires the time-dependent solution of the three-dimensional conservation equations for the neutral components. Since there is a coupling between the neutral and ionized atmospheres through ion drag processes, the similar ionospheric equations should be solved simultaneously. Although no definite method is presently available, different approaches have been summarized and discussed by several authors [see *Izakov*, 1971; *Dickinson*, 1972].

As a consequence of the difficulties which are met in establishing a realistic theoretical model, semi-empirical models are very often used for an interpretation of observational facts. Based on satellite drag data, the thermospheric models constructed by *Jacchia* [1971] have been used for a variety of applications, although they are primarily intended to give the total atmospheric density. It is therefore useful to discuss the physical meaning of such models within the framework of the three conservation equations for the mass, momentum, and energy. In the present paper, emphasis is given to the energy budget. The amount of solar energy absorbed in the thermosphere is initially considered as an unknown parameter, and it is deduced from the energy equation in such a way as to reproduce the densities and temperatures given by Jacchia's 1971 models. The deduced solar extreme ultraviolet heating is compared with theoretical calculations of absorbed energy, and reasonable agreement can only be obtained if vertical and horizontal movements are taken into account in the energy equation. In order to solve the difficulty resulting from the coupling between the ionosphere and the thermosphere, experimental incoherent scatter data are used to account for the ion-neutral interaction processes.

NUMERICAL PROCEDURE AND CONSERVATION EQUATIONS

The treatment of the three conservation equations is schematically shown in Figure 1. The solid arrows indicate the different inputs necessary for the solution of the equations and the outputs resulting from these solutions. By using Jacchia's 1971 models, horizontal pressure gradients are calculated above Saint-Santin (44°38'N, 2°13'E) as a function of height, local time, season, and solar activity. These results, combined with the ion drifts and the electron concentrations deduced from incoherent scatter data, are then used to solve the horizontal momentum equation so that the meridional and zonal neutral winds can be computed above Saint-Santin. The horizontal gradients of the meridional wind are also obtained from the solution of the momentum equation at two latitudes 2.5° north and 2.5° south of Saint-Santin. With the exception of the external heating, the terms involved in the energy equation can now be deduced. It is therefore possible to compute the external heating Q_{EXT} necessary to assure a consistent ther-

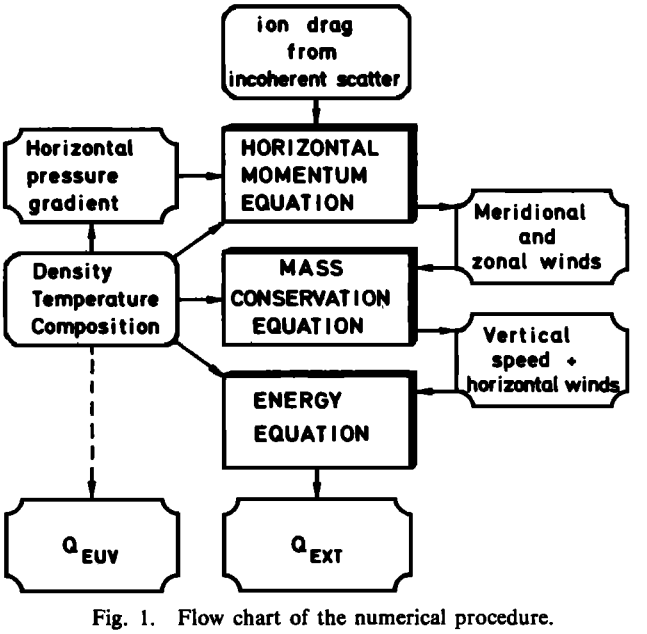

Fig. 1. Flow chart of the numerical procedure.

mal balance in Jacchia's 1971 model. The solar extreme ultraviolet heating Q_{EUV} can also be directly computed from the model (dashed arrow) by using solar EUV fluxes, relevant absorption cross sections, and a heating efficiency. A comparison can then be made between the two amounts of absorbed energy Q_{EXT} and Q_{EUV}. It is to be underlined that this local procedure cannot reach latitudinal variations of the solar heat input away from the Saint-Santin location.

The flow chart of Figure 1 has been applied above Saint-Santin for solstice and equinox conditions, a stationary state being assumed in a reference system fixed with respect to the sun, i.e., longitude and local time are equivalent. Furthermore, spherical coordinates are used, where r is the geocentric distance, θ is the colatitude, and φ is the longitude related to local time through the angular frequency ω of the earth's rotation. The two horizontal momentum equations in a rotating frame can then be written by taking the mass average velocity C(U, V, W) of the neutral gas characterized by southward U, eastward V, and upward W components:

$$\rho \frac{\partial U}{\partial t} + \rho_i \nu_{in}(U - U_i) - \frac{\partial}{\partial r}\left(\mu \frac{U}{\partial r}\right) - 2\omega V \cos\theta = -\frac{1}{r}\frac{\partial p}{\partial \theta} \quad (1)$$

and

$$\rho \frac{\partial V}{\partial t} + \rho_i \nu_{in}(V - V_i) - \frac{\partial}{\partial r}\left(\mu \frac{\partial V}{\partial r}\right) + 2\omega U \cos\theta = -\frac{1}{r \sin\theta}\frac{\partial p}{\partial \varphi} \quad (2)$$

with

$$\frac{\partial}{\partial \varphi} = \frac{1}{\omega}\frac{\partial}{\partial t}$$

In these equations, ρ is the total atmospheric density, and p is the total pressure. The subscripts i and n refer, respectively, to the ions and to the neutrals. The calculated ion density ρ_i assumes that the concentration of atomic oxygen ions is equal to the measured electron concentration. The ion-neutral collision frequency ν_{in} is obtained from *Stubbe* [1968] as

$$\nu_{in} = 9.3 \times 10^{-16}(T/1000)^{0.37} n(\mathrm{O}) + 6.9 \times 10^{-16} n(\mathrm{N_2}) \quad (3)$$

where only O^+ ions are assumed to collide with atomic oxygen and molecular nitrogen of concentrations $n(O)$ and $n(N_2)$ in units per cubic centimeter. The ion drift velocities U_i and V_i are obtained from seasonal averages of incoherent scatter data obtained in 1971–1972. The viscosity μ is computed according to the expression given by *Banks and Kockarts* [1973]:

$$\mu = AT^{0.69} \quad (4)$$

in grams per centimeter per second, where T is the absolute temperature. The coefficient A is given by

$$A = [3.9 \times 10^{-6} n(\mathrm{O}) + 3.43 \times 10^{-6} n(\mathrm{N_2})]/[n(\mathrm{O}) + n(\mathrm{N_2})] \quad (5)$$

Molecular oxygen, hydrogen, and helium are neglected, since they play no role in the height range between 200 km and 500 km, where viscosity is important.

By using the numerical method described by *Amayenc and Vasseur* [1972], (1) and (2) are integrated between 120-km and 500-km altitude. It can be seen that the nonlinear terms are not included in the equations of motion [*Bailey et al.*, 1969; *Rishbeth*, 1972], although these terms could be important during the early morning hours [*Rüster and Dudeney*, 1972]. Figure 2 shows an example of the meridional velocity U (positive southward) and the zonal velocity V (positive eastward) obtained at 300 km above Saint-Santin for fall conditions when the maximum daytime temperature in Jacchia's 1971 model was 1026°K. These velocities are comparable with the results obtained previously [see *Rishbeth*, 1972]. The differences are mainly due to various choices of the ion drag term.

When the total density continuity equation is written in spherical coordinates, it is possible to deduce the vertical velocity W from the following equation

$$\frac{\partial \rho}{\partial t} + \frac{1}{r}\frac{\partial(\rho U)}{\partial \theta} + \frac{\rho U}{rtg\theta} + \frac{1}{r \sin\theta}\frac{\partial(\rho V)}{\partial \varphi} = -\frac{\partial(\rho W)}{\partial r} \quad (6)$$

where the term $2\rho W/r$ is neglected. The terms on the left-hand side of (6) can be evaluated by using the results obtained from the momentum equation and the densities from the model. With the boundary condition $\rho W = 0$ at infinity, (6) leads to

$$\rho W = -\int_z^\infty \frac{\partial(\rho W)}{\partial r}\, dr \quad (7)$$

at any altitude z. Numerical integration is performed between height z and 500 km. From 500 km to infinity the integrals are evaluated by assuming an isothermal atmosphere with atomic oxygen as the major component. Under these conditions $\int_{500}^{\infty} \rho\, dz \simeq \rho(\mathrm{O})H(\mathrm{O})$, $H(O)$ being the atomic oxygen scale height. Furthermore, U/r and V/r are assumed to be constant at heights above 500 km. An example of the vertical velocity obtained by this procedure is shown in Figure 2. Several authors [*Dickinson and Geisler*, 1968; *Rishbeth et al.*, 1969; *Bailey and Moffett*, 1972] have separated the vertical velocity into two parts: a breathing velocity due to thermal contraction or expansion and an additional velocity arising from the convergence or divergence of air produced by horizontal winds. The vertical velocity shown in Figure 2 takes both effects into account, since no particular assumption has been made concerning the total density continuity equation.

The momentum and mass conservation equations have been used to compute the three-dimensional movements consistent with Jacchia's 1971 model. It is now possible to make a complete analysis of the energy equation, which can be written as

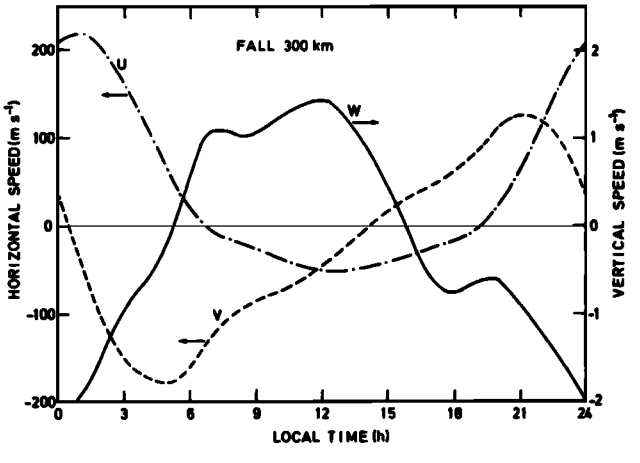

Fig. 2. Diurnal variation of the meridional wind U, of the zonal wind V, and of the vertical speed W computed at a 300-km altitude for quiet conditions during fall equinox.

follows in terms of the temperature T:

$$\rho c_v \left(\frac{\partial T}{\partial t} + \mathbf{C}\cdot\nabla T\right) + p\nabla\cdot\mathbf{C} + \nabla\cdot(-\lambda\nabla T) = Q_{EXT} - Q_{IR} + Q_V + Q_F \quad (8)$$

where p is the total pressure, c_v is the specific heat at constant volume, and λ is the thermal conductivity coefficient. On the right-hand side of (8), $-Q_{IR}$ is the loss due to the 63-μm infrared emission of atomic oxygen, Q_V is the heat dissipation due to viscosity, and Q_F is the ion-neutral friction dissipation. The infrared loss has been computed with the expression given by *Bates* [1951] for an optically thin atmosphere, although this approximation is not valid below 150 km [*Kockarts and Peetermans*, 1970]. The viscous dissipation is approximated [*Izakov*, 1971] by

$$Q_V = \mu[(\partial V/\partial r)^2 + (\partial U/\partial r)^2] \quad (9)$$

whereas the ion-neutral friction term is given by

$$Q_F = \rho_i \nu_{in} \frac{m}{m_i + m} |\mathbf{C}_i - \mathbf{C}|^2 \quad (10)$$

m being the neutral mean molecular mass. The term Q_{EXT} in (8) represents then the solar heating and any other process which could play a role in the thermal balance, such as energy exchange between the ionized and the neutral gas at different temperatures or tidal wave and gravity wave dissipation. With the exception of Q_{EXT}, all the terms in (8) can be computed from the solutions of the mass and momentum conservation equations. Using the temperature distribution given by *Jacchia* [1971], one obtains the solid curve Q_{EXT} shown in Figure 3. This is the amount of external energy required to assure the thermal balance imposed by (8). If Q_{EXT} is assumed to be the result of solar extreme ultraviolet heating, it should be compared with the amount of absorbed energy Q_{EUV} directly computed from the model (see Figure 1). Using the absorption cross sections and the 'minimum' extreme ultraviolet fluxes given by *Banks and Kockarts* [1973] below 1027 Å, one obtains the curve labelled Q_{EUV} in Figure 3 with a heating efficiency of unity. This result is comparable with the external source Q_{EXT} obtained from the energy equation for solar activity conditions $F = 125 \times 10^{-22}$ W m^{-2} Hz^{-1}, and it implies that 1.7 ergs cm^{-2} s^{-1} are converted into heat. A Q_{EUV} curve similar to that of Figure 3 can also be obtained with the 'high-average' extreme ultraviolet fluxes given by *Banks and Kockarts* [1973] if the adopted heating efficiency is 0.5, i.e., a value in agreement with *Chandra and Sinha* [1973]. In the latter case the energy available at the top of the atmosphere is 3.5 ergs cm^{-2} s^{-1}, and 1.7 ergs cm^{-2} s^{-1} are again converted into heat. If a heating efficiency $\epsilon \sim 0.3$ has to be used, as was recently suggested by *Stolarski et al.* [1975], it would be necessary to multiply the previous value of the available solar energy at the top of the atmosphere roughly by a factor of 2. The total energy flux available between 1027 and 80 Å measured by *Hinteregger* [1970] is of the order of 2.3 ergs cm^{-2} s^{-1}, whereas the results obtained on board Aeros A [*Schmidtke et al.*, 1974] lead to a value of 3.8 ergs cm^{-2} s^{-1}. Because of the uncertainty in the heating efficiency no attempt will be made to decide which set of EUV data is the more representative. The question of absolute EUV fluxes has recently been reanalyzed by *Prasad and Furman* [1974], who concluded that arguments advanced for doubling the solar fluxes measured by *Hinteregger* [1970] below 1300 Å are not compelling.

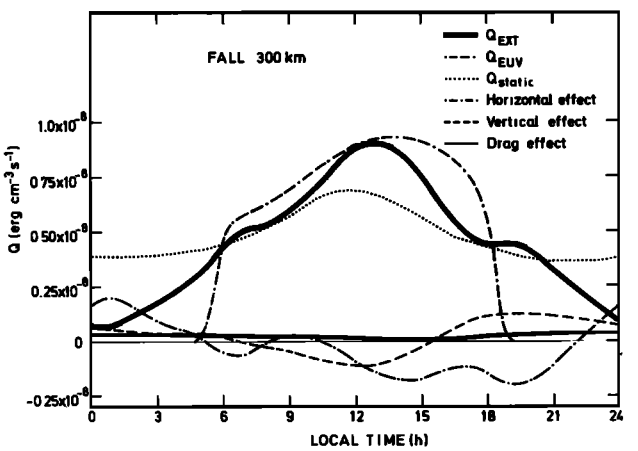

Fig. 3. Diurnal variation of the energy input Q_{EXT} and Q_{EUV} obtained by the procedure shown in Figure 1; Q_{EXT} is obtained from (8) when horizontal and vertical effects, as well as the ion drag term Q_F, are taken into account. The curve Q_{static} results from (11). The viscous heat dissipation Q_V given by (9) is found to be negligible and is therefore not indicated on the figure.

Since every term in (8) has the dimension of energy per unit volume and per unit time, it is possible to analyze, in a simple way, how the dynamical phenomena affect the energy balance. When all the terms involving a velocity are neglected in the energy equation (8), one obtains

$$\rho c_v \frac{\partial T}{\partial t} + \nabla\cdot(-\lambda\nabla T) = Q_{static} - Q_{IR} \quad (11)$$

where Q_{static} replaces the symbol Q_{EXT}. The comparison between Q_{static} and Q_{EUV} indicates in Figure 3 that without dynamical effects the sole EUV heat source would be unable to assure a thermal structure consistent with Jacchia's 1971 model. For instance, a nighttime source of approximately 4×10^{-9} erg cm^{-3} s^{-1} is required at 300 km, whereas the maximum daytime source reaches only 7×10^{-9} erg cm^{-3} s^{-1}. The difference between Q_{static} and Q_{EXT} results essentially from the horizontal and vertical movements whose effects are shown in Figure 3. The horizontal transport represents a loss process between 0900 and 2200 local time, whereas the vertical transport is equivalent to a loss process during daytime and a heat production process during nighttime. It has been shown [*Kockarts*, 1973] that these effects can be simulated, in a one-dimensional heat conduction equation, by introducing a small nighttime production and a daytime loss around 300 km.

It appears from Figure 3 that Jacchia's 1971 model is roughly consistent with solar EUV heating as the major external source if dynamical terms are included in the energy equation. This conclusion is, however, valid only above 200 km, since the evaluation of the wind system at lower heights is not sufficiently reliable. This results from the fact that Jacchia's 1971 model is mainly based on satellite drag data obtained above 200 km.

Nevertheless, some differences between Q_{EXT} and Q_{EUV} appear in Figure 3. For sunrise and sunset conditions the discrepancy could result from the omission of the nonlinear term in the momentum equation, since *Rüster and Dudeney* [1972] have shown that this term becomes more important at sunrise and at sunset.

Discussion

The computations described in this paper have been made for solstice and equinox conditions by using seasonal averages

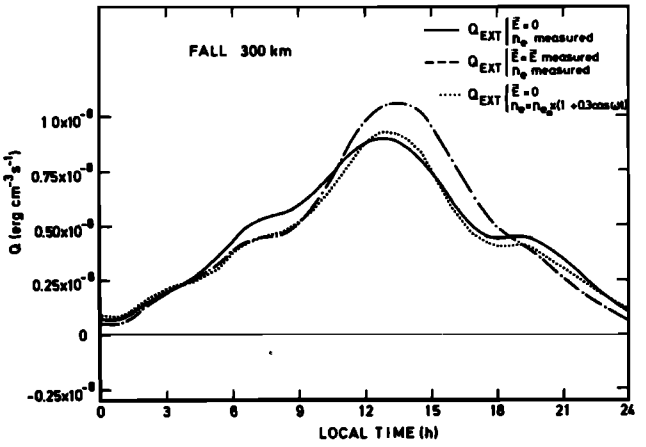

Fig. 4. Effects on Q_{EXT} resulting from modifications in the ion drag term as indicated in the text.

for the ion drifts and electron concentrations obtained at Saint-Santin in 1971–1972, when the average 10.7-cm solar flux was of the order of 125×10^{-22} W m^{-2} Hz^{-1}. The use of seasonal averages for ion drifts and electron concentrations avoids the introduction in the ion drag force of high-order Fourier terms which could appear in single-day observations. Such terms are not suitable according to the smoothed character of Jacchia's model and associated pressure gradient driving forces.

The influence of the ion-drag term deduced from experimental data can be investigated by an arbitrary modification of the measured electron concentrations. Although the meridional and zonal components of the neutral wind are sensitive to a change in the electron concentration, the thermal balance given by (8) is not greatly affected by a 30% change in the electron concentration. This can be seen in Figure 4, where the dotted curve Q_{EXT} results from the modification of the electron concentration n_e according to the arbitrary expression given in Figure 4.

In the results shown in Figures 2 and 3, only ion drift velocities parallel to the magnetic field are taken into account. It is, however, interesting to investigate the possible effect of ion drifts perpendicular to the field, which can be induced by electric fields in the F region.

The recently established quadristatic system of Saint-Santin [*Bauer et al.*, 1974] allows the determination of the perpendicular component of the ion drift. Typical results for quiet magnetic conditions [*Amayenc et al.*, 1974] indicating an electric field of up to 1–2 mV/m have been introduced in the ion drag terms of (1) and (2). The solid curve of Figure 4 is

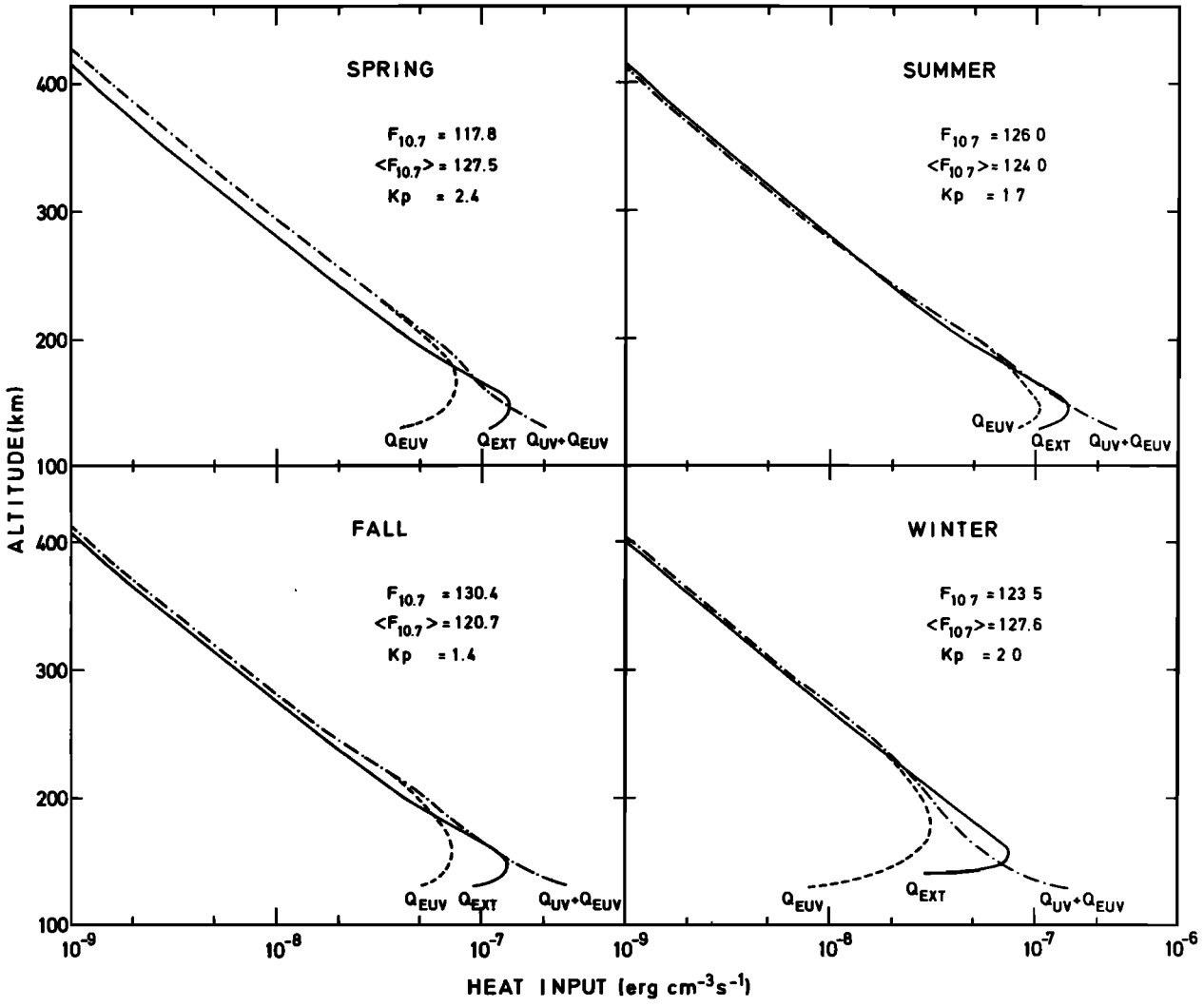

Fig. 5. Vertical distribution of heat inputs averaged over the sunlit period. The Schumann-Runge continuum is taken into account in the curves labelled $Q_{UV} + Q_{EUV}$.

now transformed into the dot-dash curve. It is to be noted that the heating due to a local electric field of the order of 1–2 mV/m does not significantly contribute to the heat balance. The difference between the two curves results almost entirely from the modification of the wind system and not from the frictional heating Q_F in (8).

It appears from Figure 4 that this difference is not very large, and in Figure 5 the vertical distribution of the theoretical heat input Q_{EUV} is compared with the heat input Q_{EXT} obtained without taking into account ion drifts perpendicular to the geomagnetic field. The solar activity conditions are indicated for each season, and the heat input profiles are time averages over the sunlit period. Below 200 km the effect of the Schumann-Runge continuum Q_{UV} has been taken into account by using the solar fluxes given by *Ackerman* [1971] and a heating efficiency of 0.3 [*Izakov*, 1971]. The agreement between Q_{EUV} and Q_{EXT} is satisfactory above 200 km for all seasons.

This agreement implies that under quiet conditions the use of *Jacchia*'s [1971] model in the three-dimensional conservation equations at medium latitude leads to a reasonable description of the global heat budget in the upper thermosphere, provided that solar EUV heating is the major source and that vertical heat conduction and dynamical redistribution processes are taken into account. Since the uncertainty in the evaluation of the dynamical effect increases below 200 km, it is, however, not necessarily correct to extrapolate the present conclusion to lower heights.

Acknowledgment. The Editor thanks R. E. Dickinson for his assistance in evaluating this report.

REFERENCES

Ackerman, M., Ultraviolet solar radiation related to mesospheric processes, in *Mesospheric Models and Related Experiments*, edited by G. Fiocco, pp. 149–159, D. Reidel, Dordrecht, Netherlands, 1971.

Amayenc, P., and G. Vasseur, Neutral winds deduced from incoherent scatter observations and their theoretical interpretation, *J. Atmos. Terr. Phys.*, *34*, 351–364, 1972.

Amayenc, P., P. Bauer, M. Blanc, C. Taieb, and J. Testud, *F* region electric fields behavior above Saint-Santin (France), paper presented at Fall Annual Meeting, AGU, San Francisco, Calif., 1974.

Bailey, G. J., and R. J. Moffett, The influence of vertical motions on the diurnal variations of the temperature and density in the thermosphere, *Planet. Space Sci.*, *20*, 1085–1094, 1972.

Bailey, G. J., R. J. Moffett, and H. Rishbeth, Solution of the coupled ion and neutral air equations in the mid-latitude ionospheric *F*2-layer, *J. Atmos. Terr. Phys.*, *31*, 253–270, 1969.

Banks, P. M., and G. Kockarts, *Aeronomy*, parts A and B, Academic, New York, 1973.

Bates, D. R., The temperature of the upper atmosphere, *Proc. Phys. Soc. London, Sect. B*, *64*, 805–821, 1951.

Bauer, P., P. Waldteufel, and C. Vialle, The French quadristatic incoherent scatter facility, *Radio Sci.*, *9*, 77–83, 1974.

Chandra, S., and A. K. Sinha, The diurnal heat budget of the thermosphere, *Planet. Space Sci.*, *21*, 593–604, 1973.

Dickinson, R. E., Dynamics of the thermosphere, *Space Res.*, *12*, 1015–1023, 1972.

Dickinson, R. E., and J. E. Geisler, Vertical motion field in the middle thermosphere from satellite drag densities, *Mon. Weather Rev.*, *96*, 606–616, 1968.

Hinteregger, H. E., The extreme ultraviolet solar spectrum and its variation during a solar cycle, *Ann. Geophys.*, *26*, 547–554, 1970.

Izakov, M. N., On theoretical models of the structure and dynamics of the earth's thermosphere, *Space Sci. Rev.*, *12*, 261–298, 1971.

Jacchia, L. G., Revised static models of the thermosphere and exosphere with empirical temperature profiles, *Spec. Rep. 332*, 113 pp., Smithson. Astrophys. Observ., Cambridge, Mass., 1971.

Kockarts, G., Heat balance and thermal conduction, in *Physics and Chemistry of Upper Atmospheres*, edited by B. M. McCormac, pp. 54–63, D. Reidel, Dordrecht, Netherlands, 1973.

Kockarts, G., and W. Peetermans, Atomic oxygen infrared emission in the earth's upper atmosphere, *Planet. Space Sci.*, *18*, 271–285, 1970.

Prasad, S. S., and D. R. Furman, Is there a real need for doubling the solar EUV fluxes?, *J. Geophys. Res.*, *79*, 2463–2468, 1974.

Rishbeth, H., Thermospheric winds and the *F* region: A review, *J. Atmos. Terr. Phys.*, *34*, 1–47, 1972.

Rishbeth, H., R. J. Moffett, and G. J. Bailey, Continuity of air motion in the mid-latitude thermosphere, *J. Atmos. Terr. Phys.*, *31*, 1035–1047, 1969.

Rüster, R., and J. R. Dudeney, The importance of the non-linear term in the equation of motion of the neutral atmosphere, *J. Atmos. Terr. Phys.*, *34*, 1075–1083, 1972.

Schmidtke, G., K. Rawer, W. Fischer, and C. Rebstock, Absolute EUV photon fluxes of aeronomic interest, paper presented at COSPAR meeting, Sao Paulo, 1974.

Stolarski, R. S., P. B. Hays, and R. G. Roble, Atmospheric heating by solar EUV radiation, *J. Geophys. Res.*, *80*, in press, 1975.

Stubbe, P., Frictional forces and collision frequencies between moving ion and neutral gases, *J. Atmos. Terr. Phys.*, *30*, 1965–1985, 1968.

(Received December 23, 1974;
revised February 24, 1975;
accepted February 26, 1975.)